Low-temperature magnetization step and its training effects in phase-separated $La_{0.5}Ca_{0.5}MnO_3$

2001 J. Phys.: Condens. Matter 13 1973

(http://iopscience.iop.org/0953-8984/13/9/319)

INSTITUTE OF PHYSICS PUBLISHING JOURNAL OF PHYSICS: CONDENSED MATTER

J. Phys.: Condens. Matter **13** (2001) 1973–1978 www.iop.org/Journals/cm PII: S0953-8984(01)19883-8

Low-temperature magnetization step and its training effects in phase-separated $La_{0.5}Ca_{0.5}MnO_3$

Run-Wei Li, Ji-Rong Sun, Qing-An Li, Zhao-Hua Cheng, Zhi-Hong Wang, Shao-Ying Zhang and Bao-Gen Shen

State Key Laboratory of Magnetism, Institute of Physics and Centre for Condensed Matter Physics, Chinese Academy of Sciences, PO Box 603, Beijing 100080, People's Republic of China

E-mail: rwli@g203.iphy.ac.cn

Received 8 December 2000, in final form 22 January 2001

Abstract

We observed a magnetization step accompanied by a metal–insulator transition around 75 K in $La_{0.5}Ca_{0.5}MnO_3$. Repeating measurements under the same condition weaken the magnetization step and enhance the resistance at low temperature. The decayed magnetization step reappears after annealing the sample at high temperature or cooling it under a magnetic field. The low-temperature magnetization step can be attributed to the melting of the overcooled ferromagnetic fragments and its training effect may be related to structure distortions at the interfaces between the ferromagnetic and charge-ordered phases in the investigated system.

1. Introduction

Hole-doped manganites $Ln_{1-x}A_xMnO_3$ (Ln = rare earth, A = alkaline earth) with a distorted perovskite structure have stimulated a considerable scientific and technological interest due to their versatile effects such as the colossal magnetoresistance [1–3], charge and orbital ordering [4–6]. Magnetoresistance effects in these compounds have been interpreted in terms of the so-called double-exchange model [7–9]. However, there are many other phenomena that cannot be explained according to the double-exchange model alone. To explain the complicated magnetic and transport behaviours observed in $Ln_{1-x}A_xMnO_3$, Moreo *et al* [10] proposed a phase separation scenario, which is supported by subsequent NMR [13, 14] and Mössbauer [15] investigations. Anane *et al* [11] found a thermal relaxation from a metastable metallic ferromagnetic (FM) phase to an insulating antiferromagnetic (AFM) phase in the charge-ordered (CO) $Pr_{0.7}Ca_{0.3}MnO_3$ single crystal, supporting the coexistence of metal and insulator phases in the compound. Uehara *et al* [12] interpreted the dramatic response of the resistance to the magnetic field in terms of the percolative phase separation in the compounds showing reduced T_C. From the scanning tunnelling spectroscopy study, Fäth *et al* [16] observed in $La_{0.7}Ca_{0.3}MnO_3$ thin film a phase separation below T_C, randomly distributed metal and insulator domains coexist and the size and structure of the domains are strongly field dependent.

0953-8984/01/091973+06$30.00

Based on the electronic microscopy observation, Mori *et al* [17] found the coexistence of FM and AFM CO microdomains with the size of 20–30 nm in $La_{0.5}Ca_{0.5}MnO_3$. It is notable that, in phase-separated compounds, there would be numerous interfaces between nano-scale FM and CO phases which can affect strongly magnetic and transport properties. In this paper, we reported a low-temperature magnetization step and its training effects in the phase-separated $La_{0.5}Ca_{0.5}MnO_3$. The low-temperature magnetization step is found to result from the overcooled metastable FM phase and its training effect may be related to the interfaces between the FM and CO phases.

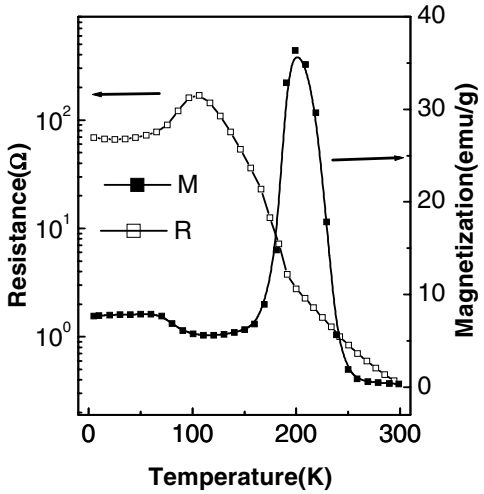

Figure 1. M–T and R–T curves for the first measurement from 5 to 300 K under a field of 0.05 T for the former and 0 T for the latter.

2. Experiment

Bulk $La_{0.5}Ca_{0.5}MnO_3$ was prepared by conventional solid-state reaction processing. The well mixed La_2O_3, $CaCO_3$ and $MnCO_3$ powders with appropriate proportion were calcinated at 800 °C for 24 h. The resulting mixture was reground, pressed into pellets and sintered at 1300 °C for 48 h. X-ray diffraction, carried out on a Rigaku x-ray diffractometer with a rotating anode and Cu Kα radiation, indicates that the sample is single phase with an orthorhombic structure. Magnetization measurements were performed on a commercial SQUID magnetometer. Resistance was measured by the standard four-probe method.

3. Results and discussions

Figure 1 displays the temperature dependence of magnetization (M–T) and resistance (R–T) of $La_{0.5}Ca_{0.5}MnO_3$. In agreement with the reports [13, 14], a paramagnetic to FM phase transition at 240 K followed by an FM to AFM charge ordering transition at 175 K are observed. An obviously discernible rise of resistance occurs around 175 K due to the onset of charge ordering. According to the phase diagram reported by Schiffer *et al* [18], $La_{1-x}Ca_xMnO_3$ is FM for $0.2 < x < 0.5$, AFM and CO for $x > 0.5$. In fact, in our sample, there exist FM metal phase embedding in the CO matrix at low temperature, which can be concluded from the high magnetization below the charge ordering transition temperature (T_{CO}). At low temperature,

the FM fraction was evaluated to be 24% [19]. Interestingly, with a further decrease of temperature, a magnetization step of about 2.2 emu g^{-1} at 75 K appears accompanied by an insulator–metal transition in the R–T curve. Xiao *et al* [20] and Yoshinari *et al* [21] observed similar behaviours; however, they did not give any explanation or further investigation. In the following, we will focus our attention on the magnetic anomaly at and below 75 K.

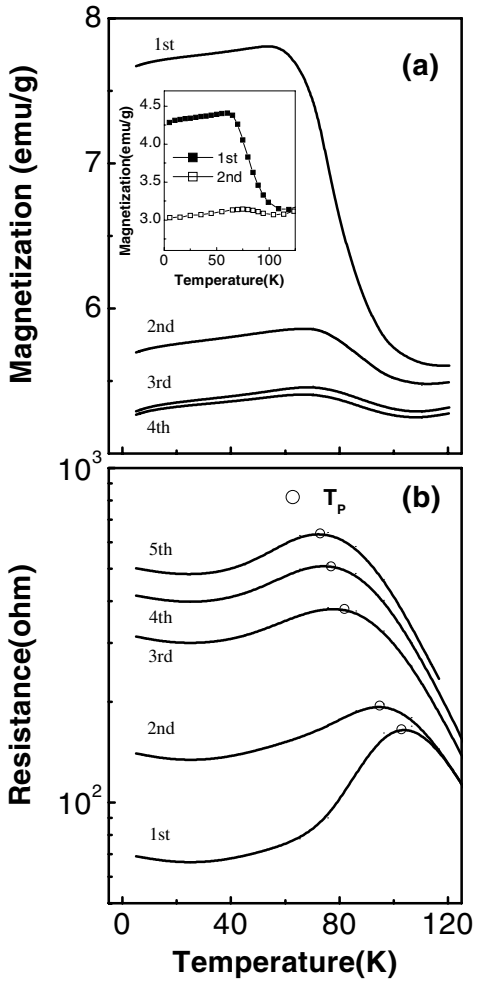

Figure 2. Magnetization under a field of 0.05T (a) and zero-field resistance (b) as a function of temperature measured by heating for many times. The inset of (a) shows the training process of the magnetization step for the sample that was annealed at 1200 °C for 3 h after many measurements had been performed.

Figure 2(a) shows the temperature dependence of magnetization measured under a field of 0.05 T. For this measurement, the sample was cooled without magnetic field (ZFC) to 5 K, then a field of 0.05 T was applied and the data were recorded by heating until 300 K. This process was repeated for several times. It is interesting that the magnetization at a fixed temperature decreases with increasing number of repeated measurements. The height of the magnetization step decreases from 2.2 emu g^{-1} for the first measurement to 0.4 emu g^{-1} for the second measurement. However, subsequent measurements reduce the step slightly and the

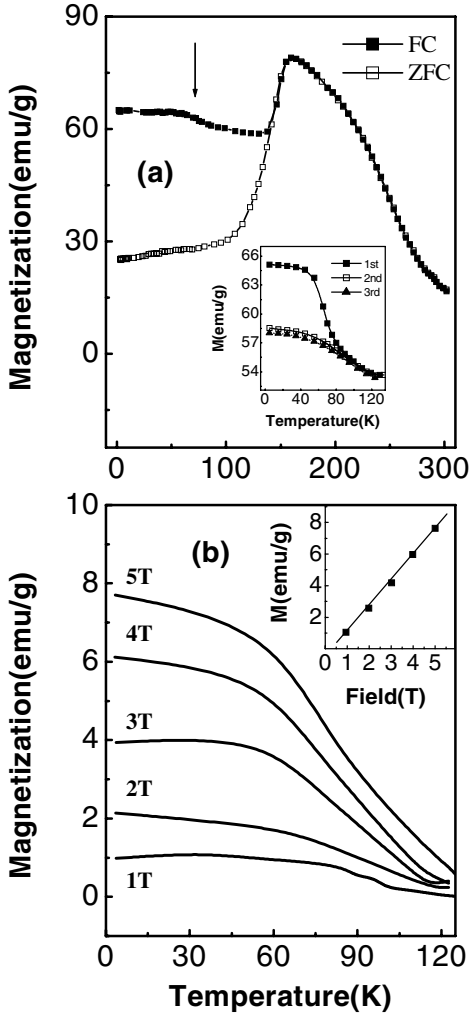

Figure 3. (a) Temperature dependence of magnetization at a field of 4 T in zero-field-cooled and field-cooled modes, respectively. (b) The net low-temperature magnetization step measured under various fields in field-cooled mode. The inset of (a) shows the training process of the field-cooled magnetization under a field of 4 T. The inset of (b) presents the height of the net step at 5 K as a function of the magnetic field.

height approaches 0.1 emu g^{-1} finally. Fascinatingly, the low-temperature magnetization step and the training effect reappear when the repeatedly measured sample is annealed at 1200 °C for 3 h in air, as shown in the inset of figure 2(a). The resistance at zero field as a function of temperature is presented in figure 2(b). The overall resistance increases especially in the low temperature region and the metal–insulator transition temperature shifts to low temperature correspondingly with the number of times measured. Comparing the M–T to R–T curves, an excellent correspondence, the decrease of magnetization corresponding to the increase of resistance, can be observed, which indicates that spin-dependent scattering plays an important role in the electron transport process.

Figure 3(a) shows the M–T curves measured under a field of 4 T in ZFC and FC (field-cooled) modes, respectively, for the sample that had been measured many times. The M–T

curves measured in different modes deviate from each other conspicuously below T_{CO}, which can be interpreted in terms of the thermally activated two-level model proposed previously for the $Nd_{0.5}Sr_{0.5}MnO_3$ system [22]. Interestingly, in the FC mode, the vanished low-temperature magnetization step due to the training process reappears, demonstrated as the magnetization enhancement in temperature range from 5 K to 75 K (figure 3(a)). However, the magnetization step cannot be observed in the ZFC mode even under a magnetic field of 6.5 T. The inset of figure 3(a) presents the FC M–T curves measured in the same condition for several times. There is a large discrepancy between the first and second measurement below 75 K, but no obvious change for the subsequent measurements. In order to clearly show the cooling field dependence of the low-temperature magnetization step, we deducted the magnetization background below T_{CO} and obtained the net magnetization step as shown in figure 3(b). The inset of figure 3(b) presents the height of the net magnetization step at 5 K as a function of the cooling field. It is clear that the height of the step increases linearly with the cooling field.

The temperature dependence of magnetization (shown in figure 4) was measured under a field of 0.05 T in cooling and warming modes, respectively, for the sample that had been measured for many times. The magnetization exhibits strong temperature hysteresis. The CO–FM transition occurs around 175 K and 125 K in warming and cooling processes, respectively, as reported in [13, 14]. In fact, the warming and cooling M–T curves deviate from each other in the temperature range from ∼75 K to 200 K (as shown in the inset of figure 4). Upon cooling, CO clusters begin to separate out from the FM matrix around 150 K, and grow gradually with the drop of temperature until 75 K. Overcooled fragments of the FM phase cannot be converted to the CO state below 75 K because the potential barrier between the FM and CO states is high enough compared to thermal fluctuation; however, it can occur above 75 K in the warming process. So the melting of the overcooled FM fragments should be responsible for the magnetization step around 75 K in warming process.

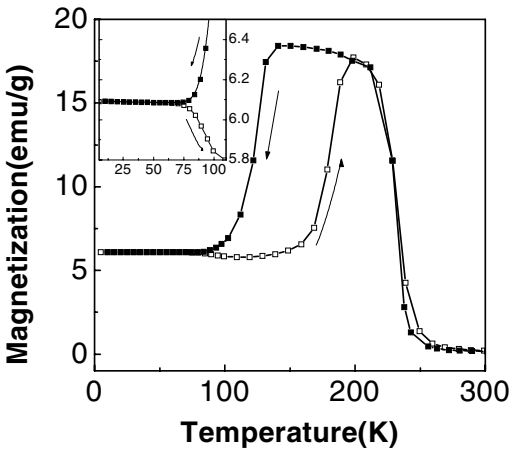

Figure 4. Temperature dependence of magnetization measured at 0.05 T in warming and cooling process.

As we known, the transition from FM to CO state occurs accompanied by a increase of lattice parameters of a and c, decrease of b and no variation of lattice volume [5, 22]. In other words, the FM and CO phases of different orthorhombic structures coexist in the phase-separated $La_{0.5}Ca_{0.5}MnO_3$. It is worth noting that significant structure distortions exist inevitably near the boundary between the FM phase and the CO one. Warming and cooling

the sample repeatedly will weaken the structure mismatch. Therefore, as an explanation, we prefer to propose that the structure distortions at the interface may be responsible for the training effects of the magnetization step and resistance at low temperature. As shown in figure 2(a), the magnetization at 5 K (related to FM phase) is 7.7 emu g^{-1} and the height of the magnetization step (related to the interface) is 2.2 emu g^{-1} under a field of 0.05 T. If the size of the FM clusters is considered as 20–30 nm, as reported in [17], a rough estimate indicates that an interface of 10–15 Å thick can cause a magnetization step of 2.2 emu g^{-1}.

4. Conclusion

By magnetic and electrical measurements, the low-temperature magnetization step was observed and ascribed to the melting of overcooled FM fragments. Numerous structure distortions at the interface between the FM phase and the CO one are proposed to be responsible for the training effects of low-temperature magnetization and resistance. It should be emphasized that more efforts should be devoted to the interfaces between different phases due to their effects on magnetic and transport properties in the phase-separated compound.

Acknowledgment

Acknowledgment will go to T S Ning and S Y Fan for their help for the measurements. This work was supported by National Natural Science Foundation of China and State Key Program of Basic Research of China.

References

[1] Jin S, Tiefel T H, McCormack M, Fastnacht R A, Ramesh R and Chen L H 1994 *Science* **264** 413
[2] Von Helmolt R, Wecker J, Holzapfel B, Schultz L and Samwer K 1993 *Phys. Rev. Lett.* **71** 2331
[3] Sun J R, Rao G H and Liang J K 1997 *Appl. Phys. Lett.* **70** 1900
[4] Mori S, Chen C H and Cheong S-W 1998 *Nature* **392** 473
[5] Kuwahara H, Tomioka Y, Asamitsu A, Moritomo Y and Tokura Y 1995 *Science* **270** 961
[6] Tomioka Y, Asamitsu A, Moritomo Y, Kuwahara H and Tokura Y 1997 *Phys. Rev. Lett.* **74** 5108
[7] Zener C 1951 *Phys. Rev.* **82** 403
[8] Anderson P W and Hasegawa H 1955 *Phys. Rev.* **100** 675
[9] de Gennes P-G 1960 *Phys. Rev.* **118** 141
[10] Moreo A, Yunoki S and Dagotto E 1999 *Science* **283** 2034
[11] Anane A, Renard J-P, Reversat L, Dupas C, Veillet P, Viret M, Pinsard L and Revcolevschi A 1999 *Phys. Rev.* B **59** 771
[12] Uehara M, Mori S, Chen C H and Cheong S-W 1999 *Nature* **399** 560
[13] Papavassiliou G, Fardis M, Belesi M, Maris T G, Kallias G, Pissas M, Niarchos D, Dimitropoulos C and Dolinsek J 2000 *Phys. Rev. Lett.* **84** 761
[14] Dho J, Kim I and Lee S 1999 *Phys. Rev.* B **60** 14 545
[15] Kallias G, Pissas M, Devlin E, Simopoulos A and Niarchos D 1999 *Phys. Rev.* B **59** 1272
[16] Fäth M, Freisem S, Menovsky A A, Tomioka Y, Aarts J and Mydosh J A 1999 *Science* **285** 1540
[17] Mori S, Chen C H and Cheong S-W 1998 *Phys. Rev. Lett.* **81** 3972
[18] Schiffer P, Ramirez A P, Bao W and Cheong S-W 1995 *Phys. Rev. Lett.* **75** 3339
[19] Li R W, Sun J R, Wang Z H, Chen X, Zhang S Y and Shen B G 2000 *Chin. Phys.* **9** 630
[20] Gang Xiao, Gong G Q, Canedy C L, McNiff E J Jr and Gupta A 1997 *J. Appl. Phys.* **81** 5324
[21] Yoshinari Y, Hummel P C, Thompson J D and Cheong S-W 1999 *Phys. Rev.* B **60** 9275
[22] Radaeli P G, Cox D E, Marezio M, Cheong S-W, Schiffer P E and Ramirez A P 1995 *Phys. Rev. Lett.* **75** 4488